Electronic and Chemical Properties of Tin-Doped Indium Oxide (ITO) Surfaces and ITO/ZnPc Interfaces Studied In-situ by Photoelectron Spectroscopy

Yvonne Gassenbauer and Andreas Klein*

Darmstadt University of Technology, Institute of Materials Science, Surface Science Division, Petersenstrasse 23, D-64287 Darmstadt, Germany

Received: November 16, 2005; In Final Form: January 10, 2006

The chemical and electronic properties of tin-doped indium oxide (ITO) surfaces and its interface with zinc phthalocyanine (ZnPc) were investigated using photoelectron spectroscopy partly excited by synchrotron radiation from the BESSY II storage ring. Preparation and analysis of ITO and ITO/ZnPc layer sequences were performed in-situ without breaking vacuum. The Fermi level position at the ITO surface varies strongly with oxygen content in the sputter gas, which is attributed to an increase of surface band bending as a consequence of the passivation of the metallic surface states of ITO. The shift of the Fermi level is accompanied by a parallel increase of the work function from 4.4 to ∼5.2 eV. No changes in the surface dipole are observed with an ionization potential of $I_P = 7.65 \pm 0.1$ eV. The barrier height for hole injection at the ITO/ZnPc interface does not vary with initial ITO work function, which can be related to different chemical reactivities at the interface.

1. Introduction

With the rising development of organic light emitting diodes (OLEDs)[1,2] and organic photovoltaic cells (OPVs),[3,4] the interest in long time stability of such devices becomes an increasing factor for commercial use. As interfaces play a crucial role for device functionality and stability, the contact between electrodes and the functional material is of big concern. To understand the influence of the electrode material on the degradation mechanisms, fundamentals of the used electrodes and their interfaces have to be known. Here, we focus on the properties of tin-doped indium oxide (ITO) which is the transparent conducting oxide (TCO) mostly used as the hole injection electrode in such devices due to its outstanding optical and electronic properties.[5,6] For Sn contents not too high, ITO adopts the bixbyite lattice structure of In_2O_3.[7]

Zinc phthalocyanine (ZnPc) is a well-studied organic material used in organic optoelectronic devices, partially in direct contact to ITO.[8−10] In addition, the distinct ZnPc C 1s core-level emission, makes it very sensitive to chemical changes and therefore suitable for interface experiments where interface reactions may play a role. High thermal stability, simple synthesis, and simple film preparation by thermal evaporation are other advantages of using ZnPc in interface experiments. A sketch of the structures of ITO and ZnPc is presented in Figure 1.

It is generally accepted that an increase in the ITO work function by an oxidative treatment leads to a lower injection barrier for holes.[11−15] Because of its degenerate doping, ITO is usually treated like a metal and the increase in work function is consequently attributed to an increase in the surface dipole, leaving the position of the Fermi level with respect to the band edges unaffected. However, ITO is a semiconductor where the Fermi level position at the surface and in the bulk can be different.[16−18] In general, the change of the work function is then given by the sum of the changes in surface dipole and in the Fermi level position at the surface. Although it is possible to differentiate between the two contributions using photoelectron spectroscopy, which allows for a direct determination of work function and Fermi level position, the individual contributions to the increase of ITO work function are not resolved. Work on In_2O_3 suggests that the increase in work function is solely due to a change in Fermi level position.[17]

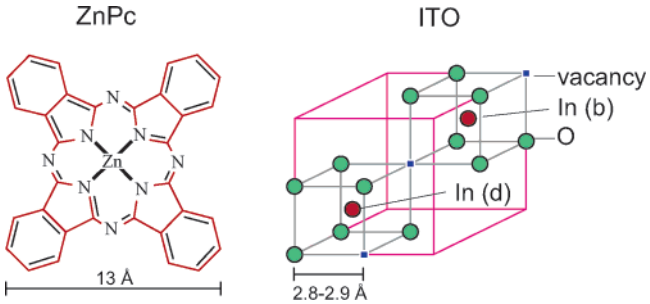

Figure 1. Sketch of the molecular structure of ZnPc. A simplified section of the unit cell of ITO neglecting relaxation of the oxygen atoms from their corner positions is shown on the right. The distance between the oxygen atoms varies between 2.8 and 2.9 Å.[7]

Work functions and Fermi level positions at semiconductor surfaces are easily affected by surface contamination. Contamination effects, however, can be avoided if the surface properties are investigated without breaking vacuum. In this paper, we describe the chemical and electronic properties of ITO surfaces and ITO/ZnPc interfaces studied using photoelectron spectroscopy. The aim of this study is to identify variations of the surface electronic properties of ITO with deposition conditions and to correlate them with variations in the interface formation with organic materials. The possibility to avoid exposing the substrate to air and humidity before deposition of the organic material will provide further insight into the "intrinsic" properties of the interfaces.

* To whom correspondence should be addressed. E-mail: aklein@surface.tu-darmstadt.de.

10.1021/jp056640b CCC: $33.50 © 2006 American Chemical Society
Published on Web 02/15/2006

The paper mainly consists of two parts. First, surface and bulk properties of radio frequency magnetron sputtered ITO thin films and their modification using different Ar/O_2 sputter gas mixtures are presented. In the second part, studies of interfaces between two differently prepared ITO samples and the organic semiconductor ZnPc are described.

2. Experimental Section

In the present study, ITO thin films were deposited using a radio frequency (rf) magnetron sputtering from a ceramic target (90 wt % In_2O_3 and 10 wt % SnO_2) in a custom-designed UHV chamber. The deposition chamber has a base pressure of 5×10^{-9} mbar and is equipped with planar magnetrons powered by a tuning network and a 13.56 MHz rf power supply (Huettinger). The power density was adjusted to 0.62 W/cm^2, and the gas flow and gas mixture (Ar, O_2) were set using leak valves to a total pressure of 5×10^{-3} mbar during deposition. Before deposition, the target was presputtered for 1 h. The target-to-sample distance was 7 cm. All films were deposited at 400 °C substrate temperature onto fluorine-doped SnO_2-coated glass substrates. The substrates were heated to 400 °C for 1 h before deposition in order to reach thermal equilibrium. The ITO deposition time was 1 h for all samples resulting in 300−600 nm thick polycrystalline films depending on the gas mixture. After the deposition was finished, the gas supply was closed and the samples were cooled to room temperature.

X-ray diffraction performed in standard Bragg−Brentano geometry revealed only bixbyite lattice reflections with a pronounced (222) texture of ITO films deposited with 10% oxygen in the sputter gas. A less pronounced texture with preferred (440) orientation is obtained for films deposited with pure Ar. Scanning force microscopy reveals multicrystalline surfaces with grain sizes of ∼200 nm. The average surface roughness of the films is ∼4 and ∼1.7 nm for films deposited with pure Ar and with 10% oxygen, respectively.

Differently prepared ITO thin films were analyzed in the DAISY-MAT system (DArmstadt Integrated SYstem for MA-Terials research), which combines several deposition and surface treatment chambers with a multitechnique surface analysis system (Physical Electronics PHI 5700) by an ultrahigh vacuum transfer.[19] X-ray photoelectron spectra were recorded using monochromatic Al Kα radiation at an overall resolution of 400 meV. Binding energies were calibrated by setting the Ag 3d binding energy to 386.27 eV. UP spectra were excited by a helium discharge lamp ($h\nu = 21.22$ eV) and recorded in normal emission with a sample bias of −1.5 eV. The work functions were determined by the mean position of the secondary electron cutoff, which has a typical broadening of less than 200 meV.

Two ITO/ZnPc interfaces were investigated with ITO substrates deposited either with pure Ar or with a gas mixture of 90% Ar and 10% O_2. The different substrates for interface experiments were in the following indicated as ITO:Ar and ITO:O_2, respectively. Organic films were grown by thermal evaporation onto the freshly prepared ITO substrates using homemade effusion cells built with resistively heated Al_2O_3 crucibles. The substrates were held at room temperature during growth. After each deposition step, the samples were characterized using photoelectron spectroscopy. To enhance sensitivity at low coverage, synchrotron radiation was used as the excitation source for the interface measurements. The deposition chamber was directly connected to the SOLIAS (SOlid LIquid Analysis System) photoelectron spectrometer which operates at a base pressure of 10^{-10} mbar.[20] The spectrometer was attached to the U49/2 PGM II undulator beamline, which provides photons in the energy range 90−1300 eV from the synchrotron facility BESSY II in Berlin.[21] Binding energies were calibrated with respect to a Au Fermi edge. Valence band spectra and secondary electron cutoffs were recorded at 150 eV excitation energy and a sample bias of −5 V. The thickness of the ZnPc films was calculated assuming layer-by-layer growth using the attenuation of the core-level lines which were normalized with respect to the electron current in the storage ring. A photoelectron escape depth of 8 Å was used,[22] which corresponds to the kinetic energies of 160 and 70 eV of the recorded In 3d and O 1s lines.

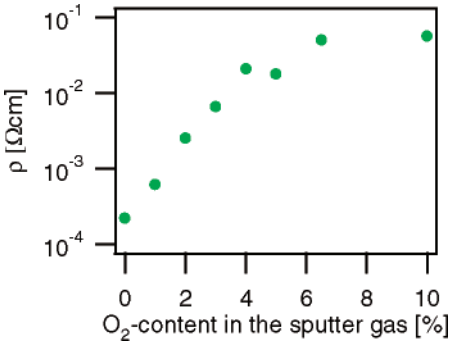

Figure 2. Resistivity of ITO thin films as a function of oxygen content in the sputter gas. The substrate temperature was 400 °C for all samples.

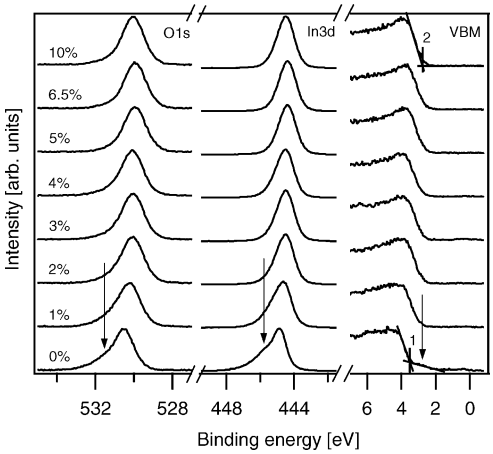

Figure 3. Al Kα excited X-ray photoelectron core-level and valence band spectra of ITO thin films prepared with varying oxygen content in the sputter gas. All samples were deposited with a 400 °C substrate temperature. The arrows and numbers refer to features described in the text.

3. Properties of ITO Films

Electrical resistivities measured by the four-point probe method in linear contact geometry of ITO thin films, which were deposited with 0−10% O_2 in the sputter gas onto quartz substrates, are shown in Figure 2. When no oxygen is present, a minimum resistivity of about 2×10^{-4} Ω cm is reached, which is close to the optimum value reported for this material.[5,6,23] The low resistivity provides clear evidence for highly degenerate n-type doping, which is further proven by observation of the Burstein−Moss shift as reported earlier for comparable samples.[16] With increasing oxygen content, the resistivity increases continuously up to a saturation value of $\sim 5 \times 10^{-2}$ Ω cm.

O 1s and In 3d XPS emission lines and valence band spectra are shown in Figure 3. Almost symmetric core-level line shapes and a well-defined valence band maximum are observed for the film deposited with 10% O_2. With decreasing oxygen content in the sputter gas (more reducing conditions), the O 1s and In 3d core-level emission lines develop a shoulder on the high

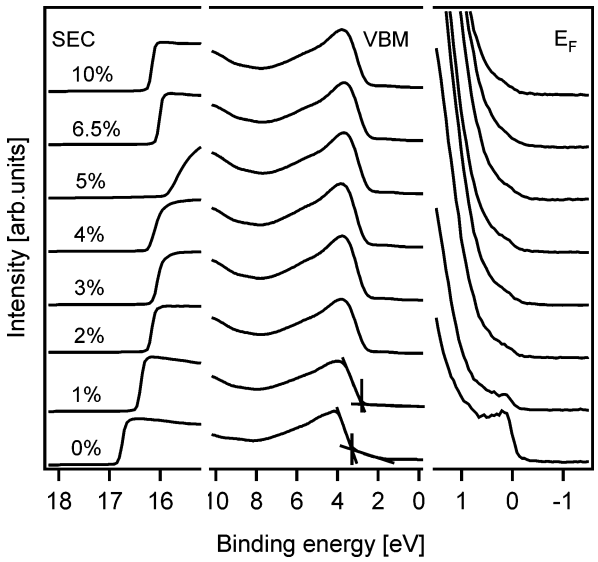

Figure 4. UP spectra of the same ITO thin films prepared with varying oxygen content in the sputter gas. All samples were deposited at a 400 °C substrate temperature.

binding energy side, as indicated by arrows in Figure 3. Although the observed shoulders could be explained by chemically shifted components,[10,24] this most likely does not apply here as XPS survey spectra show only In, Sn, and O emission lines, indicating that the surfaces are free of any noticeable contaminations. The presence of hydroxides, which would not be directly observed using XPS, is also not very likely as these should not depend as strongly on the sputter gas composition. In addition, hydroxides should result in noticeable UPS emissions at binding energies 7−10 eV.[25] Such emissions are not observed as evident from Figure 4.

We attribute the shoulders observed in the core level spectra to inelastic losses of the photoelectrons due to scattering with surface plasmons, which only occur for high carrier concentration at the surfaces.[26−28] Therefore, the shape of the core-levels changes with oxygen content in the sputter gas due to changes of the electron concentration at the surface. The plasmon energy of degenerate ITO is typically 0.5−1 eV,[5,26] in good agreement with the energy difference between the main emission line and the observed shoulder. Since the shape of the emission lines changes with oxygen content, the derivation of binding energies will depend on the details of the model used for explaining the line shapes. Throughout this paper, core-level binding energies were derived from minima of the second derivatives of the emission lines. These values deviate by less than 50 meV from values of the binding energy of the bulk emission component derived using a sophisticated fitting routine[27] and will therefore not significantly affect the presented result.

Films deposited in pure Ar show emissions above the valence band maximum at binding energies 2−3.5 eV (also indicated by an arrow in Figure 3). Such states are frequently observed at reduced oxide surfaces and are typically attributed to incomplete coordination of surface cation species.[17,27−30] The binding energies of the valence band maxima BE(VB) were determined by the intersection of the linear extrapolation of the low binding energy edge (see "2" in Figure 3). The band gap states observed in the valence band spectra of the films prepared under most reducing conditions (0% O_2) are treated as a background emission, which was subtracted when determining the valence band maximum (see "1" in Figure 3). Since the energy distribution of the band gap states is not known, the background is simply approximated by a straight line.

Increasing the oxygen content in the sputter gas leads to a binding energy shift of all core levels and the valence band maximum to lower energies. The energetic position of the Fermi level with respect to the band edges can be directly determined from the valence band maximum binding energy BE(VB), as zero binding energy corresponds to the position of the Fermi level. A higher oxygen content in the sputter gas therefore obviously leads to a lower Fermi energy position. This would correspond to a lower doping level, which is also indicated by an increase of resistivity. A lower doping level with increasing oxygen content is expected as surplus oxygen is known to compensate substitutional Sn_{In} donors by forming neutral defect complexes [$2Sn_{In}O_i$], which are known to be the most abundant point defect in ITO.[31,32] The sample prepared under most reducing conditions (100% Ar) shows a valence band maximum at BE(VB) = 3.3 eV, which is slightly smaller than the band gap of 3.6 eV.[5] Consequently, the Fermi level is near the conduction band edge but not inside the conduction band as it would be expected for degenerate behavior (see also discussion in ref 27).

Ultraviolet photoelectron spectra (UPS) of the different samples are shown in Figure 4. Different intensity scales are applied for different binding energy regions in order to highlight the important features of the spectra. A Fermi edge (E_F) emission is clearly identified for films deposited with no or little oxygen content in the sputter gas in agreement with the literature.[12,19,26,27,33] The Fermi edge emission has been attributed to metallic surface states rather than to filled conduction band states.[19,27] The intensity of the emissions at the Fermi edge is strongly reduced with increasing oxygen content. No Fermi edge emission is identified for strongest oxidizing conditions. Addition of oxygen to the sputter gas therefore either leads to a strong reduction of the density of surface states or to a shift of the Fermi level position to an energy where no or only very few surface states exist.

The band gap states for most reducing conditions are also observed in UPS valence bands as evident from the central part of Figure 4. Compared to valence bands measured using XPS (see Figure 3), the UPS valence bands show a higher intensity at a binding energy of about 4 eV. The different shape is due to the different energy dependence of the photoionization cross sections of the O 2p and In 4d states,[34] which both contribute to the valence band states.[35] At lower excitation energies, the O 2p contributions dominate the spectrum, and at higher excitation energies, the In 4d states contribute significantly. That O 2p states dominate the spectrum at a binding energy of ∼4 eV is also indicated by the increase of intensity at ∼4 eV in the XPS valence bands with increasing oxygen content in the sputter gas (see Figure 3).

The left part of Figure 4 shows the secondary electron cutoffs (SECs). An increase in work function with increasing oxygen content is evident, in agreement with the increased work function observed after oxidative surface treatments.[11−13] The magnitude of the work function shift is the same as the shift of the valence band maximum. Both values are shown in Figure 5 depending on the oxygen content in the sputter gas. The almost parallel run indicates that the energy shift is only caused by a shift of the Fermi level. No significant change of the surface dipole is observed. Work functions above 5 eV are observed for all films deposited with ≥2% O_2 in the sputter gas (no work function is given for the sample deposited with 5% O_2 because of the atypical shape of the cutoff).

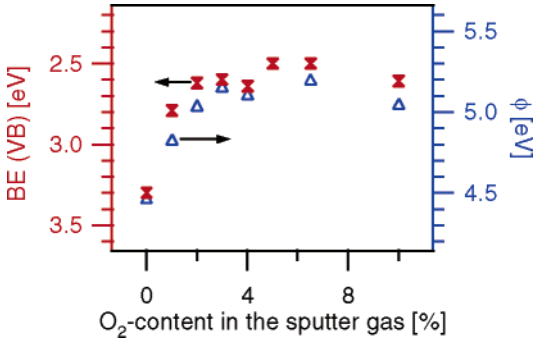

Figure 5. Binding energy of the valence band maximum BE(VB) and work function ϕ depending on the oxygen content in the sputter gas. The values were determined from the UP spectra.

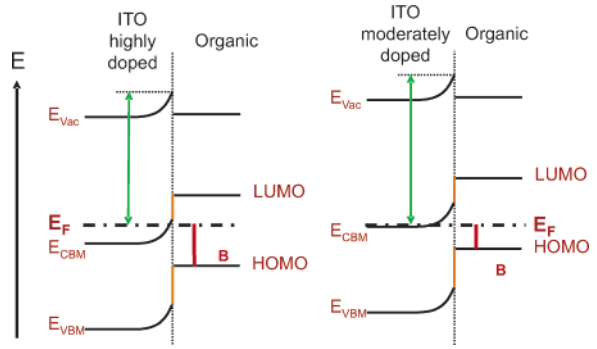

Figure 6. Hypothetic band lineups between ITO and an organic semiconductor. The ITO on the left side is highly doped whereas the ITO on the right side exhibits a lower doping and should lead to a smaller barrier height for hole injection.

4. ITO/ZnPc Interfaces

The observations presented in the previous section affect the understanding of the function of ITO electrodes in organic devices. Two schematic examples, where differently prepared ITO films are in contact with an organic semiconductor, are shown in Figure 6. Since the barrier height for hole injection Φ_B, given by the distance between the Fermi energy and the highest occupied molecular orbital (HOMO) level of the organic semiconductor, is modified by the work function,[11−15] it is expected to change with ITO deposition conditions. Highly doped ITO:Ar deposited with pure Argon leads to a certain barrier height for hole injection. In the case of the moderately doped ITO:O_2 deposited using additional oxygen, the work function is larger since the valence band maximum is closer to the Fermi level. Consequently, a lower barrier height is expected. The following sections will show how the preparation of ITO affects the interface formation and the barrier height at the ITO/ZnPc interface.

4.1. ITO Prepared with Pure Ar. Figure 7 shows valence band photoemission spectra of the ITO:Ar/ZnPc interface recorded with 150 eV photon energy. The bottom spectrum in the series shows the freshly prepared 600 nm thick ITO:Ar film. The In 4d emission line at a binding energy of (BE $\approx$ 18 eV) has a comparatively low intensity which is due to a low photoionization cross section at 150 eV photon energy.[34] The intensity of the In 4d line decreases with ZnPc coverage, while the Zn 3d emission line at BE $\sim$ 11 eV increases. The O 2p derived valence band states between 3 and 10 eV BE gradually change to the molecular orbitals of ZnPc, including its HOMO level at BE $\approx$ 1.5 eV. The spectral region of the Fermi level and the HOMO level is shown on a larger scale in the insert.

A Fermi edge emission is observed for the ITO:Ar substrate as shown in the insert. It is attenuated but does not disappear

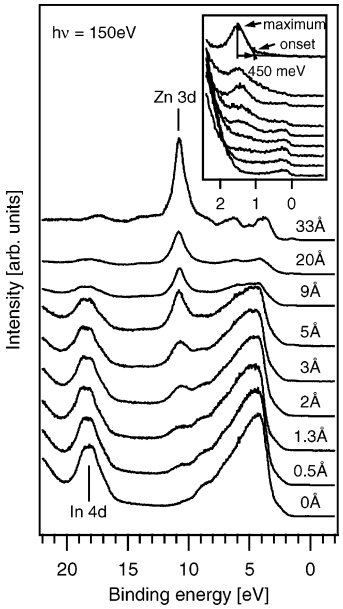

Figure 7. Valence band spectra of an ITO/ZnPc interface where the ITO was sputtered with pure Ar. The excitation energy was 150 eV. The insert shows the region around the Fermi edge and HOMO level, respectively, in more detail.

with initial ZnPc deposition, indicating that the associated surface states[27] are not passivated by the deposition of ZnPc molecules. The same holds for the emissions from electronic surface states above the ITO valence band maximum. Inspection of the valence band states therefore indicates that there is no strong chemical interaction between ZnPc and ITO:Ar. For thick coverage, the onset of the HOMO is measured at $HOMO_{onset} = 1.04 \pm 0.05$ eV and the maximum of the HOMO level at $HOMO_{max} = 1.49 \pm 0.05$ eV. A work function of 4.14 ± 0.1 eV is determined for thick coverage. The width of the HOMO level, the work function, and the ionization potential of the ZnPc film are in good agreement with the literature.[8,36,37]

Figure 8 shows corresponding C 1s and O 1s core-level spectra measured with excitation energies of 450 and 600 eV, respectively. The intensities were normalized to the peak maximum to make the chemical shifts and line shapes more evident. The C 1s emission spectra reflect the development of the ZnPc layer. For the highest film thickness, the C 1s spectrum is composed of a strong emission at 284.8 eV binding energy accompanied by a second emission shifted by 1.4 eV and a third emission shifted by 3.2 eV to higher binding energy. This is the typical shape of the C 1s emission of phthalocyanines reported in the literature, which is composed of the emission from the two chemically different carbon atoms in ZnPc and a $\pi-\pi^*$ satellite (see Figure 1).[38,39] With a ZnPc thickness of $\sim$2 Å, the C 1s emission line exhibits a line shape, which compares well with the characteristic emission structure of ZnPc. However, at lower coverage, the C 1s emission is significantly broadened, which has also been observed by others and been attributed to charge-transfer processes rather than to chemical decomposition of the molecules.[39] The straight line indicates the final position of the C 1s intensity maximum. It is drawn to show that there are only small binding energy shifts with increasing film thickness. Nitrogen 1s emissions, which have also been recorded (not shown), show a behavior comparable to that of the C 1s emission. No different chemical components are identified. The binding energy shifts are also in parallel to those of the C 1s line.

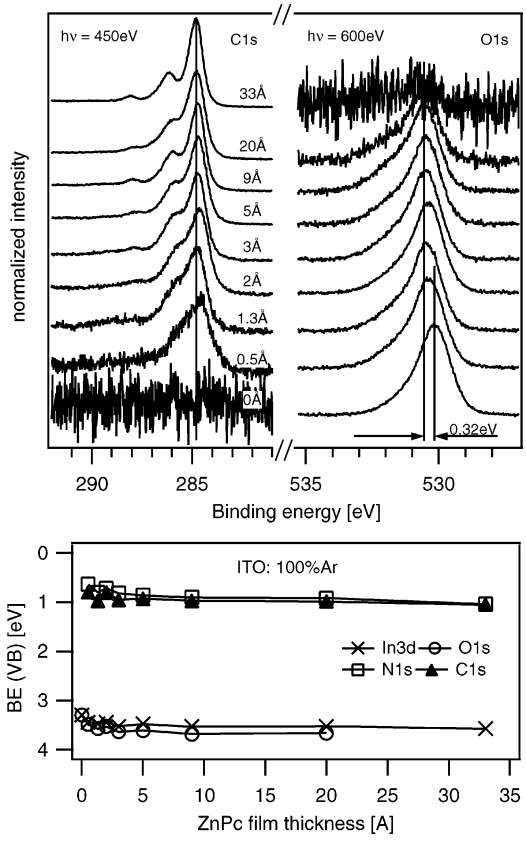

Figure 8. (top) Normalized C 1s and O 1s core-level spectra of an ITO/ZnPc interface. The ITO was sputtered with pure Ar. The excitation energy was set to 450 eV for C 1s and 600 eV for O 1s, respectively. (bottom) Valence band and $HOMO_{onset}$ positions determined from core-level binding energies as a function of ZnPc film thickness.

The O 1s emission lines in Figure 8 reflect the changes of the ITO:Ar substrate. It exhibits a shift to higher binding energies, mainly after the first deposition step. Further deposition of ZnPc leads only to small shifts of the O 1s binding energy, which are in parallel to the shifts of the C 1s line. The total binding energy difference between the pure ITO:Ar substrate and the last detectable O 1s emission amounts to 0.37 ± 0.05 eV. A comparable shift of 0.28 ± 0.05 eV is observed in the In 3d emission, indicating a Fermi level shift in the ITO:Ar substrate as the origin for the binding energy shift. The average shift of the O 1s and the In 3d level is given by 0.32 eV.

The evolution of the core-level binding energies with ZnPc thickness is displayed in the bottom part of Figure 8. The binding energy differences between a particular core level and the valence band maximum or the onset of the HOMO level ($BE_{VB,HOMO}(CL) = BE(CL) - BE(VB, HOMO_{onset})$) are subtracted from the binding energies. The $BE_{VB,HOMO}(CL)$ are determined from valence band and core-level spectra of the ITO:Ar substrate and the thick ZnPc layer, respectively. The same photon energies were used for valence band and core-level spectra in each case. The corresponding $BE_{VB,HOMO}(CL)$ values can be determined with a typical uncertainty of $\approx \pm 0.1$ eV and are given as $BE_{VB}(In3d_{5_2}) = 441.43$ eV, $BE_{VB}(O1s) = 526.88$ eV, $BE_{HOMO}(C1s) = 284.19$ eV, and $BE_{HOMO}(N1s) = 397.88$ eV, respectively. Assuming that these values do not change with interface formation, the changes of the core-level binding energies reflect the changes of the valence band maximum and $HOMO_{max}$ position with respect to the Fermi energy depending on ZnPc coverage.

To construct a band diagram, additional electronic properties not accessible from photoelectron spectroscopy have to be known. Preceding characterization by optical spectroscopy of ITO films prepared under identical conditions indicates that, assuming a bulk band gap of 3.6 eV,[5] the bulk Fermi level position prepared under the same conditions lies 0.7 eV above the conduction band minimum E_{CBM}.[16] Accordingly, there is a large difference between the bulk and surface Fermi level position of ~1 eV, which is partially reduced with deposition of ZnPc. The barrier for hole injection Φ_B is given by the distance between the onset of the HOMO level and the Fermi level and amounts to 1.04 ± 0.05 eV. The determined interface dipole potential δ, determined from the difference of vacuum energies at the interface as $\delta = 0.31 \pm 0.1$ eV, is of a similar magnitude than that for other ITO/organic interfaces.[39,40] A complete band diagram is shown in Figure 9. The included lowest unoccupied molecular orbital (LUMO) position is derived from the energetic distance between the maximum of the HOMO and the LUMO levels in ZnPc as measured by photoelectron spectroscopy and inverse photoelectron spectroscopy, which amounts to 3 eV.[41]

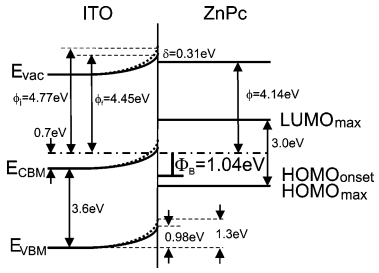

Figure 9. ITO/ZnPc band diagram where the ITO was sputtered with pure Ar. The barrier for hole injection Φ_B is 1.04 ± 0.1 eV. An interface dipole potential of -0.31 ± 0.1 eV is present at the interface. Dotted lines mark the initial ITO electronic properties.

4.2. ITO Prepared with 10% O_2. For ITO films deposited with the addition of oxygen in the sputter gas, the resulting higher work function predicts a lower barrier height for hole injection. The particular ITO:O_2 film which is used here as the substrate for ZnPc deposition has been deposited using 10% O_2. Figure 10 shows corresponding valence band spectra in the course of ZnPc deposition. The binding energy region around the Fermi energy and the HOMO level is shown in the insert. In agreement with the results described in section 3, the uncovered ITO:O_2 film exhibits a lower binding energy of the valence band maximum compared to the ITO:Ar film and no emission at the Fermi energy is observed. However, as soon as ZnPc is deposited on the surface, a large shift of the valence band toward higher binding energies is observed and a Fermi edge appears. The valence band spectrum of the thick ZnPc agrees with the one presented in the previous section and represents an undisturbed thick ZnPc layer with comparable HOMO and Zn 3d emissions and also an identical width of the HOMO level of 0.45 eV.

The C 1s and O 1s core levels recorded during interface formation are shown in Figure 11. The characteristic three components of the C 1s emission are not observed until a thick ZnPc layer is deposited. For the first evaporation step, the ZnPc C 1s emission lines consist of a broad main line at a binding energy expected for the main emission from ZnPc molecules and an additional peak at a binding energy of 289.4 eV, which is characteristic for carboxyl groups.[42] Since carbon is present only from the deposited ZnPc molecules, the C 1s emission structure clearly indicates an oxidation of the deposited molecules with a disintegration of the ZnPc structure, that is, breaking of C−C or C−N bonds. The chemical reaction is less evident in the O 1s spectra which can be explained by (i) the

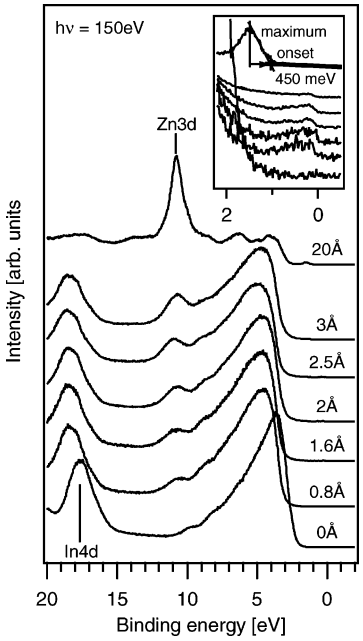

Figure 10. Valence band spectra of an ITO/ZnPc interface where the ITO was sputtered with a gas mixture of 90% Ar and 10% O_2. The excitation energy was 150 eV. The insert shows the region around the Fermi level and HOMO level, respectively, in more detail.

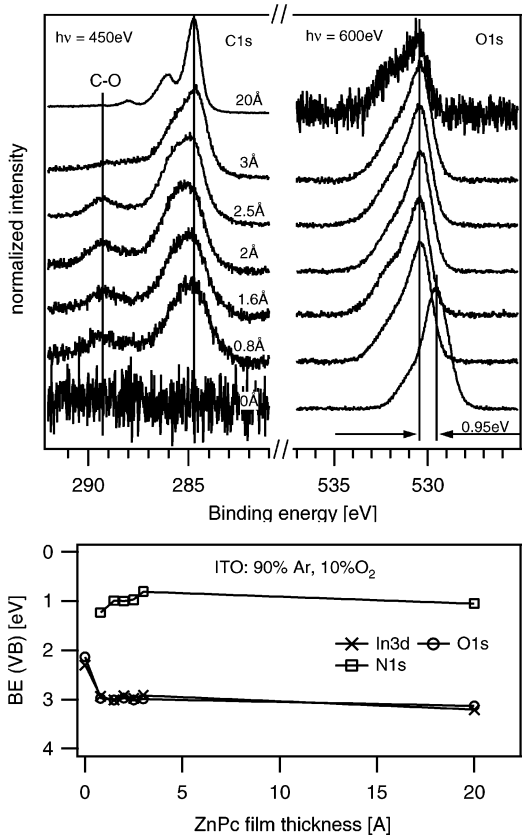

Figure 11. (top) Normalized C 1s and O 1s core-level spectra of an ITO/ZnPc interface. The ITO was sputtered with 90% Ar and 10% O_2. The excitation energy was set to 450 eV for C 1s and 600 eV for O 1s, respectively. (bottom) Valence band and $HOMO_{onset}$ positions determined from core-level binding energies as a function of ZnPc film thickness.

low concentration of reacted species (spectra in Figure 11 are normalized in intensity), (ii) the binding energy of oxygen in carboxyl groups is in the same region as those of the shoulders

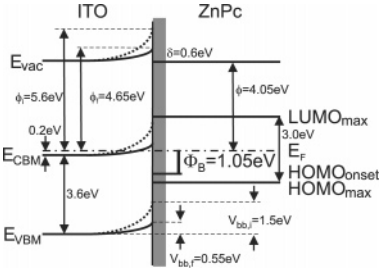

Figure 12. ITO/ZnPc band diagram where the ITO was sputtered with 90% Ar and 10% O_2. The barrier for hole injection ϕ_B is 1.05 ± 0.1 eV. An interface dipole of −0.6 ± 0.1 eV is present at the interface. As an interface reaction takes place, the ZnPc band positions are not well defined for low film thickness, which is indicated by the shadowed bar. Dotted lines mark the initial ITO electronic properties.

of the O 1s peak of the ITO substrate,[42] and (iii) the shape of the O 1s peak can change also as a result of the energy shift which occurs after the first ZnPc deposition step (see section 3). The N 1s emissions (not shown) also show a strong broadening at low coverage.

The evolution of the ITO valence band maximum and ZnPc HOMO level onset is shown at the bottom part of Figure 11. No values for $HOMO_{onset}$ can be derived from the C 1s core level as the line shape for low coverage is not characteristic for ZnPc. The distance between the $HOMO_{onset}$ and the N 1s core emission of the thick ZnPc film amounts to 397.81 ± 0.1 eV, which is in good agreement with the experiment described in the previous section. The binding energies of the ITO core levels with respect to the valence band maximum for the clean ITO:O_2 substrate are $BE_{VB}(In3d_{5/2})$ = 441.91 ± 0.1 eV and $BE_{VB}(O1s)$ = 527.44 ± 0.1 eV. Both values are ∼500 meV larger than the values for ITO:Ar. This unusual behavior is reproducibly observed for ITO films prepared under the respective conditions. The different values for BE_{VB} can be attributed to screening of the photoemission core hole by the high concentration of electrons in surface states. A detailed description of the experimental observations and its origin are given in ref 27. The explanation given therein for the variation of BE_{VB} with deposition conditions is supported by the reduction of BE_{VB} of the ITO:O_2 film by ∼0.25 eV with the deposition of ZnPc, which is determined from the data presented here. Since the Fermi edge emission reappears after the deposition of ZnPc (see insert in Figure 10), the associated metallic surface states contribute to the screening of the core level after ZnPc deposition, thereby reducing their binding energies.

The binding energy shift of the In 3d line amounts to 0.91 ± 0.05 eV with ZnPc deposition, that of the O 1s line to 0.99 ± 0.05 eV, giving an average value of 0.95 eV. Most of this binding energy shift is observed after the first ZnPc deposition step. Only small shifts can be observed with further ZnPc deposition. The evolution of the N 1s core level is not in parallel to the shifts of the ITO:O_2 substrate, which is also most likely attributed to the chemical decomposition of the ZnPc molecules at low coverage.

Figure 12 shows the resulting band diagram. As an interface reaction takes place, the HOMO level is not well defined for thin ZnPc coverage, which is indicated by the shadowed bar in Figure 12. The barrier for hole injection at the ITO:O_2/ZnPc interface is determined by the onset of the HOMO emission at higher coverage and amounts to 1.05 ± 0.1 eV, which is the same as that for the ITO:Ar/ZnPc interface presented above. The Fermi level positions at the ITO surfaces after ZnPc deposition are also comparable in both experiments.

5. Discussion

5.1. Chemical Properties. The presented experiments demonstrate the complexity of the ITO surfaces and their influence on interface formation with organic molecules. One important feature is that the surface of highly conducting ITO is metallic not because of electrons inside the conduction band as expected for a degenerate semiconductor but because of the presence of metallic surface states. This is extensively discussed elsewhere[27] and supported by the data presented here. A surplus of oxygen during sputter deposition of ITO results in a poorer conductivity of the material which is attributed to a compensation mechanism including the formation of neutral $[2Sn_{In}O_i]$ defect complexes. The compensation of donors leads to a reduced doping, which is accompanied by a lower Fermi level position in the bulk, which can be deduced from a red-shifted absorption edge due to the reduction of the Burstein−Moss shift.[16] The addition of oxygen to the sputter gas further leads to a strong shift of the surface Fermi level and to suppression of the Fermi edge emission. Although it cannot be distinguished, if the disappearance of the Fermi edge is due to the elimination of surface states or just due to the movement of the Fermi level, it is likely that additional oxygen atoms or molecules adsorbed on the surface strongly reduce the number of surface states. This is in agreement with the interpretation of the effect of oxidative treatments of ITO surfaces.[12,14]

The interaction of ZnPc with oxygen can occur in different ways. Huisman et al. have reported on the reversible formation of oxygen radical anions $O_2^{-\bullet}$ when ZnPc films are exposed to illumination in air by a charge transfer from photoexcited ZnPc LUMO states to oxygen molecules incorporated in the films.[43] They assume that the positive charge is most likely located on the central Zn atom. Such a mechanism does not occur here as it would not result in the formation of carboxyl groups. The chemical interaction between ZnPc and ITO here involves oxygen from the ITO substrate, and it leads to a disintegration of the structure of the ZnPc molecules. Because spectral changes are also observed in the N 1s spectra, the decomposition of the molecule most likely occurs by breaking C−N bonds.

The decomposition of the ZnPc molecules with the ITO obviously depends on the substrate preparation. A chemical decomposition of the ZnPc molecules is only evident for the ITO substrate when prepared with the addition of oxygen to the sputter gas. Most likely, oxygen adsorbed on the surface is then consumed to react with ZnPc. This is indicated (i) by the observation of carboxyl species in the C 1s core level, (ii) by the appearance of a Fermi edge emission on the ITO:O_2 surface after ZnPc deposition, and (iii) by the absence of noticeable C−O components for deposition onto ITO:Ar. Hence, an ITO:Ar surface, which has a large number of surface states due to unsaturated In atoms, does not react. A sketch of the different surfaces and their reactivity is given in Figure 13.

Literature on the chemical interaction of organic molecules with differently treated ITO surfaces is scarce. Most of the photoemission studies focus on the determination of barrier heights largely using only UPS. However, the results presented here are in agreement with the known literature. Chemical interactions at the ITO/Cu−phthalocyanine interfaces are reported by Peisert et al.[39] They discuss bond formation and charge-transfer interactions of adsorbed molecules, indicating that their deposited CuPc molecules are not decomposed on the substrate. Their C 1s core levels are similar to the ones presented here for the ITO:Ar substrate. Obviously, the surfaces of the ITO substrate used by Peisert et al. are not strongly oxidized, which is also not expected since the surfaces were prepared by sputter cleaning in a vacuum. In another UPS study of the ITO/ZnPc interface, no evidence for interface reactions is reported.[8] This, however, does also not disagree with the presented results as the valence band spectra of the ITO used by Blochwitz et al. show a strong band gap emission indicating a highly reduced surface.

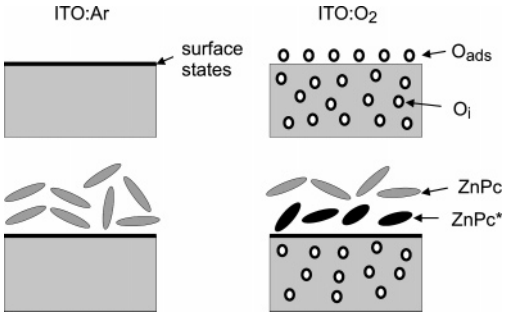

Figure 13. Sketch of the essential features of ITO films (top) and ITO/ZnPc interfaces (bottom) as determined from the present experiments. Films sputter deposited in pure Ar show a high density of surface states. Deposited ZnPc molecules do not strongly interact with the ITO surface and therefore do not considerably alter the surface states. Films deposited with oxygen in the sputter gas have a lower conductivity due the incorporation of oxygen in the films forming neutral $[2Sn_{In}O_i]$ defect complexes.[31,32] The surface states are passivated by adsorbed oxygen. With the deposition of ZnPc, the adsorbed oxygen is removed from the surface and reacts with the deposited molecules (ZnPc*). Due to the removal of the passivating oxygen, the surface states reappear.

Le et al. reported on the interaction of *N*,*N*-8-bis-(1-naphthyl)-*N*,*N*-8-diphenyl-1,18-biphenyl-4,48-diamine (NPB) with differently treated ITO surfaces.[44] Again, no chemical reaction occurs for untreated ITO. A chemical reaction occurs only for acid-treated ITO, which is explained by adsorption of acid molecules on the treated ITO surface. The acid treatment leads to an increase of the ITO work function. In agreement with the data presented here, a strong reduction of work function occurs after initial NPB deposition, which has been related to the interface reaction. Although no changes in the valence band maximum are reported by Le et al., the situation is similar to the present strong shift of the surface potential for the reactive interface, since a shift in the Fermi level position should be accompanied by a shift in work function.[45]

The reactivity at the interfaces between organic molecules and "standard" oxidatively treated ITO surfaces remains an open question. In contrast to the presented results, such treatments are known to lead to reduced barriers for hole injections.[11−15] This suggests that no chemical decomposition of organic molecules occurs on such surfaces. It is therefore suggested that the structure of such treated ITO surfaces is different from those of our ITO:O_2 films. The differences are not clear so far. In contrast, there are similarities between surfaces of our ITO:O_2 films and "standard" oxidatively treated ITO surfaces: A comparable passivation of surface states after reactive oxygen treatment is indicated by the reported reduction of the Fermi edge emission on the latter surfaces.[12] Also, the work functions of oxidatively treated ITO surfaces and of films prepared with a surplus of O_2 are of the same magnitude. Unfortunately, the Fermi level position at treated ITO surfaces is usually not given in the literature, which makes a more detailed comparison based on the available data impossible.

5.2. Electronic Properties. From the analysis of the XPS and UPS data, it is evident that the Fermi level position on ITO surfaces and interfaces can vary by almost 1 eV depending on preparation and treatment. In addition, the data in Figure 5 indicate that changes in the Fermi level position result in changes

in the work function by the same amount. This result holds at least for sputter deposited films analyzed in-situ by photoelectron spectroscopy. The parallel shift of the Fermi level and work function denotes a constant surface dipole, that is, a constant difference between vacuum level and valence band maximum. The same behavior is also observed for In_2O_3 films prepared either by reactive evaporation of In[17] or by rf magnetron sputtering.[46] However, while the ionization potential of the In_2O_3 films amounts to $I_P = 7.15 \pm 0.1$ eV, we find values of $I_P = 7.65 \pm 0.1$ eV for ITO. To our knowledge, no values are given in the literature for comparison. Differences in the electronic structure of In_2O_3 and ITO surfaces are also reflected by the absence of noticeable Fermi edge emissions at surfaces of In_2O_3 films.[27,46] Although it seems reasonable to attribute the differences to the presence of Sn, the underlying mechanism cannot be resolved with the available data.

Adding oxygen during ITO deposition is technologically not reasonable to increase the work function of ITO as it also reduces the conductivity of the films. Nevertheless, the effect on the surface potentials might be similar to those of typically performed UV ozone or oxygen plasma treatments of highly conductive ITO films, which are expected to change only the surface region. At least the work functions obtained after UV ozone or oxygen plasma treatments are of the same magnitude as those reported here for the ITO:O_2 films.[11,12,15] However, it remains unclear how these treatments affect the Fermi level position at the surface, since typically only work function changes are reported in the literature. In addition, treatments are in most cases performed ex-situ and even short air exposure might alter the surface potentials.

It is evident that the surface and interface properties of ITO generally have to be treated like those of semiconductors rather than like those of metals. Considering only the changes in work function for metals does not give an appropriate description. The apparent difference in surface and bulk Fermi level positions, the latter being derived from optical absorption spectra and electrical conductivities, has been attributed to a carrier depletion near the surface.[16,27] Since such depletion layers are not very likely for degenerately doped semiconductors, or at least extent only a few angstroms, the different Fermi level position has been related to a doping gradient in the near surface region.[18] This is in agreement with observations of increased oxygen content in nanocrystalline ITO particles.[32] More evidence for the existence of the surface depletion layers and details on the surface properties of ITO are reported elsewhere.[27]

Compared to conventional semiconductor surfaces and interfaces, ITO shows an additional complexity. While the binding energy difference between core levels and the valence band maximum BE_{VB} are generally treated as constant for a material and during an interface experiment if no chemical reaction occurs,[47,48] the BE_{VB} values of ITO differ by up to 0.5 eV as discussed in detail in ref 27. The variation can be explained by a reduced binding energy of the core hole due to screening of free electrons in the surface states.[27] In the case of the interface experiment with the ITO:O_2 substrate, a drop of In 3d to the valence band maximum distance of about 250 meV is observed, supporting this assertion. Thus, in contrast to conventional semiconductors, there is no 1:1 correlation between the Fermi level position and the core-level binding energies for ITO and most likely also for other degenerately doped semiconductors.

ZnPc valence band spectra directly provide the position of the HOMO level, which can be attributed to the barrier height for hole injection. On the basis of our results, the injection barrier is the same for both substrates, regardless of the large differences in ITO work function. The interface reaction removes adsorbed oxygen and leads to a large shift of the Fermi level at the substrate surface, which is accompanied by a reduction of the work function by the same amount. Hence, a large work function of the ITO substrate is not sufficient to reach a low injection barrier. It must also remain stable during deposition of organic materials. The ex-situ oxidative treatments of ITO as UV ozone and oxygen plasma treatments, which are assumed to have a similar effect on the passivation of surface states and increase in work function, lead to a lowering of the injection barrier,[11,14] while the in-situ addition of oxygen during the sputter deposition of ITO does not. This discrepancy warrants further investigations, in particular as a change in barrier height during operation might provide an explanation for degradation mechanisms in OLEDs.

Concerning the absolute values of the injection barriers, it is noted that different characterization techniques lead to different HOMO−LUMO gaps in organic molecules having their origins in the various electronic polarization of materials, which cannot be avoided during measurement (see discussion in ref 36 and references therein). For organic semiconductors, these effects can reach values of 1 eV and more and might result in a barrier height for hole injection determined from current transport which deviates from the one determined by photoemission.

Summary and Conclusions

We have presented a study of surface properties of ITO and its interface formation with the organic conductor ZnPc, where the complete deposition sequence and interface analysis with photoelectron spectroscopy is performed without breaking vacuum. It is shown that ITO surfaces can exhibit large Fermi level shifts depending on substrate preparation. In the particular case where ITO films are prepared by magnetron sputtering from ceramic ITO targets with different oxygen content in the sputter gas, the Fermi level shifts are accompanied by changes in work function of the same magnitude, thus leaving the ionization potential unchanged with $I_P = 7.65$ eV. Films deposited with pure Ar as the sputter gas have a work function of $\phi = 4.4$ eV and exhibit a high density of surface states. The increase in ITO work function up to $\phi = 5.2$ eV when oxygen is added to the sputter gas is enabled by a passivation of electronic surface states by adsorption of oxygen. The resulting surface can easily react with deposited organic molecules. Consequently, the passivation of the surface states is removed and the Fermi level is strongly shifted toward the conduction band, corresponding to a significant lowering of the work function. The resulting interface therefore shows a HOMO position of the organic molecule, which does not depend on the work function of the ITO substrate.

Acknowledgment. We thank D. Ensling, A. Thissen, and P. Hoffmann for help during the BESSY beamtime and T. Mayer and U. Weiler for helpful discussions and for providing us with highly purified ZnPc molecules, manufactured in the group of D. Wöhrle in Bremen. The presented work is supported by the German Science Foundation within the collaborative research center Electrical fatigue in functional materials (SFB 595).

References and Notes

(1) Dodabalapur, A. *Solid State Commun.* **1997**, *102*, 259.
(2) Hung, L. S.; Chen, C. H. *Mater. Sci. Eng., R* **2002**, *39*, 143.
(3) Brabec, C. J.; Sariciftci, N. S.; Hummelen, J. C. *Adv. Funct. Mater.* **2001**, *11*, 15.

(4) Peumans, P.; Yakimov, A.; Forrest, S. R. *J. Appl. Phys.* **2003**, *93*, 3693.
(5) Hamberg, I.; Granqvist, C. G. *J. Appl. Phys.* **1986**, *60*, R123.
(6) Hartnagel, H. L.; Dawar, A. L.; Jain, A. K.; Jagadish, C. *Semiconducting Transparent Thin Films*; Institute of Physics Publishing: Bristol, U.K., 1995.
(7) Marezio, M. *Acta Crystallogr.* **1966**, *20*, 723.
(8) Blochwitz, J.; Fritz, T.; Pfeiffer, M.; Leo, K.; Alloway, D. M.; Lee, P. A.; Armstrong, N. R. *Org. Electron.* **2001**, *2*, 97.
(9) Chan, C.; Gao, W.; Kahn, A. *J. Vac. Sci. Technol., A* **2004**, *22*, 1488.
(10) Armstrong, N. R.; Carter, C.; Donley, C.; Simmonds, A.; Lee, P.; Brumbach, M.; Kippelen, B.; Domercq, B.; Yoo, S. *Thin Solid Films* **2003**, *445*, 342.
(11) Kugler, T.; Salaneck, W. R.; Rost, H.; Holmes, A. B. *Chem. Phys. Lett.* **1999**, *310*, 391.
(12) Mason, M. G.; Hung, L. S.; Tang, C. W.; Lee, S. T.; Wong, K. W.; Wang, M. *J. Appl. Phys.* **1999**, *86*, 1688.
(13) Sugiyama, K.; Ishii, H.; Ouchi, Y.; Seki, K. *Appl. Phys.* **2000**, *87*, 295.
(14) Hill, I. G.; Milliron, D.; Schwartz, J.; Kahn, A. *Appl. Surf. Sci.* **2000**, *166*, 354.
(15) Schlaf, R.; Murata, H.; Kafafi, Z. H. *J. Electron Spectrosc. Relat. Phenom.* **2001**, *120*, 149.
(16) Gassenbauer, Y.; Klein, A. *Solid State Ionics* **2004**, *173*, 141.
(17) Klein, A. *Appl. Phys. Lett.* **2000**, *77*, 2009.
(18) Klein, A. *Mater. Res. Soc. Symp. Proc.* **2001**, *666*, F1.10.
(19) Ensling, D.; Thissen, A.; Gassenbauer, Y.; Klein, A.; Jaegermann, W. *Adv. Eng. Mater.* **2005**, *7*, 945.
(20) Mayer, T.; Lebedev, M.; Hunger, R.; Jaegermann, W. *J. Phys. Chem. B* **2006**, *110* (5), 2293−2301.
(21) Batchelor, D. R.; Follath, R.; Schmeisser, D. *Nucl. Instr. Methods Phys. Res., Sect. A* **2001**, *467*, 470.
(22) Tanuma, S.; Powell, C. J.; Penn, D. R. *Surf. Interface Anal.* **1991**, *17*, 927.
(23) Ohta, H.; Orita, M.; Hirano, M.; Hosono, H. *J. Appl. Phys.* **2002**, *91*, 3547.
(24) Donley, C.; Dunphy, D.; Paine, D.; Carter, C.; Nebesny, K.; Lee, P.; Alloway, D.; Armstrong, N. R. *Langmuir* **2002**, *18* 450.
(25) Mayer, T.; Jaegermann, W. In *Landolt Börnstein*; Springer-Verlag: Berlin-Heidelberg, Germany, 2005; Vol. III/42a (4).
(26) Christou, V.; Etchells, M.; Renault, O.; Dobson, P. J.; Salata, O. V.; Beamson, G.; Egdell, R. G. *J. Appl. Phys.* **2000**, *88*, 5180.
(27) Gassenbauer, Y.; Schafranek, R.; Klein, A.; Zafeiratos, S.; Häveckeer, M.; Knop-Gericke, A.; Schlögl, R., submitted for publication.
(28) Egdell, R. G.; Rebane, J.; Walker, T. J.; Law, D. S. L. *Phys. Rev. B* **1999**, *59*, 1792.
(29) Cox, D. F.; Fryberger, T. B.; Semancik, S. *Phys. Rev. B* **1988**, *38*, 2072.
(30) Themlin, J. M.; Sporken, R.; Darville, J.; Caudano, R.; Gilles, J. M.; Johnson, R. L. *Phys. Rev. B* **1990**, *42*, 11914.
(31) (a) Frank, G.; Köstlin, H. *Appl. Phys. A* **1982**, *27*, 197. (b) Hwang, J.-H.; Edwards, D. D.; Kammler, D. R.; Mason, T. O. *Solid State Ionics* **2000**, *129*, 135. (c) Warschkow, O.; Ellis, D. E.; González, G. B.; Mason, T. O. *J. Am. Ceram. Soc.* **2003**, *86*, 1700.
(32) González, G. B.; Mason, T. O.; Quintana, J. P.; Warschkow, O.; Ellis, D. E.; Hwang, J.-H.; Hodges, J. P. *J. Appl. Phys.* **2004**, *96*, 3912.
(33) Cox, P. A.; Flavell, W. R.; Egdell, R. G. *J. Solid State Chem.* **1987**, *68*, 340.
(34) Yeh, J. J.; Lindau, I. *At. Data Nucl. Data Tables* **1985**, *32*, 2.
(35) McGuinness, C.; Stagarescu, C. B.; Ryan, P. J.; Downes, J. E.; Fu, D.; Smith, K. E.; Egdell, R. G. *Phys. Rev. B* **2003**, *68*, 165104.
(36) Weiler, U.; Mayer, T.; Jaegermann, W.; Kelting, C.; Schlettwein, D.; Makarov, S.; Wöhrle, D. *J. Phys. Chem. B* **2004**, *108*, 19398.
(37) Schlaf, R.; Parkinson, B. A.; Lee, P. A.; Nebesny, K. W.; Armstrong, N. R. *J. Phys. Chem. B* **1999**, *103*, 2984.
(38) The particular three-component structure of the C 1s emission line is only resolved if purified ZnPc starting material is used for deposition.
(39) Peisert, H.; Knupfer, M.; Schwieger, T.; Fink, J. *Appl. Phys. Lett.* **2002**, *80*, 2916.
(40) Ishii, H.; Sugiyama, K.; Ito, E.; Seki, K. *Adv. Mater.* **1999**, *11*, 605.
(41) Kahn, A.; Koch, N.; Gao, W. Y. *J. Polym. Sci., Part B: Polym. Phys.* **2003**, *41*, 2529.
(42) See the online database of XPS binding energies of the National Institute of Standards; URL: http://srdata.nist.gov/xps/2006.
(43) Huisman, C. L.; Goossens, A.; Schoonman, J. *J. Phys. Chem. B* **2002**, *106*, 10578.
(44) Le, Q. T.; Nüesch, F.; Rothberg, L. J.; Forsythe, E. W.; Gao, Y. *Appl. Phys. Lett.* **1999**, *75*, 1357.
(45) We have also carried out experiments on the interfaces of α−NPD, which is comparable to NPB. Although an interface reaction is not as clear as for ZnPc in the core levels, a strong shift of the Fermi level is also observed for ITO substrates prepared with oxygen in the sputter gas.
(46) Schafranek, R.; Klein, A. Unpublished work.
(47) Kraut, E. A.; Grant, R. W.; Waldrop, J. R.; Kowalczyk, S. P. *Phys. Rev. B* **1983**, *28*, 1965.
(48) Capasso, F.; Margaritondo, G. *Heterojunction Band Discontinuities*; North-Holland: Amsterdam, The Netherlands, 1987.